Available online at www.sciencedirect.com
SCIENCE DIRECT®
Physica A 369 (2006) 100–121
PHYSICA A
www.elsevier.com/locate/physa

Biological physics in four lectures and three applications

M. Schick

Physics Department, Box 351560, University of Washington, Seattle, WA 98195, USA

Available online 2 May 2006

Abstract

An introduction to Biological Physics is provided by three applications of Statistical Mechanics to current problems of biological interest. They are the possibility of lateral phase separation in the plasma membrane, the design of a vesicle sensitive to its environment which could be used for drug delivery, and the process of fusion of biological membranes.

Keywords: Biological physics; Phase separation; Rafts; Drug delivery; Membrane fusion

1. Introduction

Once more. Say you are in the country; in some high land of lakes. Take almost any path you please, and ten to one it carries you down in a dale, and leaves you there by a pool in the stream. There is magic in it. Let the most absent-minded of men be plunged in his deepest reveries- stand that man on his legs, set his feet a-going, and he will infallibly lead you to water, if water there be in all that region. Should you ever be athirst in the great American desert, try this experiment, if your caravan happen to be supplied with a metaphysical professor. Yes, as every one knows, meditation and water are wedded for ever.

Ch. 1, Moby Dick

Biological Physics has become an enormously diverse, and fruitful, area of study. It has provided the field of Physics with a host of difficult and intriguing problems, from the motion of individual motor proteins to the organization of entire cells, while Physics has provided, in its turn, a clarifying, quantitative, and predictive approach to these problems which has often been lacking. There is no way that I could possibly traverse the provinces of this discipline. Instead I shall try to give a flavor of this discipline from work that I have carried out in the last several years.

It is clear to any physicist who has interacted with a biologist that the world view of these two communities is quite different. I would summarize it as follows; Given a collection of objects, a physicist would ask what is common to them; a biologist would ask what distinguishes them. Each point of view has its strengths and its weaknesses. In particular, the physicist, in his desire to cut away what he believes to be unnecessary complications, has to ask himself whether he is not eliminating the very essence of the problem. This question is, of course, at the heart of a theoretical physicist's favorite pastime; model building. Again, I hope that the tension between simplicity and complexity emerges from these lectures.

E-mail address: schick@phys.washington.edu.

0378-4371/$ - see front matter
doi:10.1016/j.physa.2006.04.009

To the students who might read these notes, I will add the personal observation that working in Biological Physics provides the opportunity to interact with others in many other disciplines, some of whom think like you, and some who do not. The interactions are often maddening and frustrating, but they are equally likely to be stimulating and rewarding. I have found the ratio of the latter to the former to be large enough, and the whole enterprise brings me a great deal of pleasure.

1.1. First lecture: Introduction to the self-organization of amphiphiles

In the first lecture, I shall introduce some of the molecules with which I shall be dealing, namely, various lipids. After a brief description, I shall turn to their most interesting feature, their ability to assemble themselves into various structures. The most interesting structure, biologically, is the lipid bilayer. I will then set a seemingly simple task; to calculate the areal density of lipids in such a bilayer. This will illustrate some of the difficulties inherent in a description of these systems.

1.1.1. Lipids

Lipids consist of a hydrophilic head group and, usually, two hydrophobic hydrocarbon tails. The two are connected to a backbone, often the simple three-carbon molecule glycerol, $HOCH_2CH(OH)CH_2OH$. These, then, are called glycerolipids. So let us start with the head group. We remove one OH group from one of the carbons at the end of the chain of three in glycerol (we'll call this position 3) and one H from phosphate, H_2PO_4 and put them together, then remove the remaining H from the phosphate and an OH from some alcohol ROH to make the headgroup RPO_4 which is attached at position 3 on the backbone. (see Fig. 1.) One of the oxygens is ionized and thus is negatively charged. What molecule R is distinguishes the headgroup. Two of the most common are ethanolamine, $CH_2CH_2N^+H_3$, and choline, $CH_2CH_2N^+(CH_3)_3$ which give these lipids their names of phosphatidylethanolamine and phosphatidylcholine. I note two things. First, the head groups, with the negatively charged oxygen and the positively charged nitrogen, have a dipole which interacts with the dipoles of water. Second, the choline is significantly bigger than the ethanolamine as one has replaced each of the H attached to the nitrogen by the much larger methyl group, CH_3. The effects of this difference in architecture will appear often.

Now to the tails. We make them from fatty acids of the form $CH_3(CH_2)_xCOOH$ and attach them to the glycerol backbone at positions 1 and 2 by removing the OHs from the glycerol and the H from the acid. The chains are distinguished by their number of carbons, and whether they are saturated, as in the formula for the fatty acid I gave above, or whether they are unsaturated, that is, have any double bonds. Usually, but not

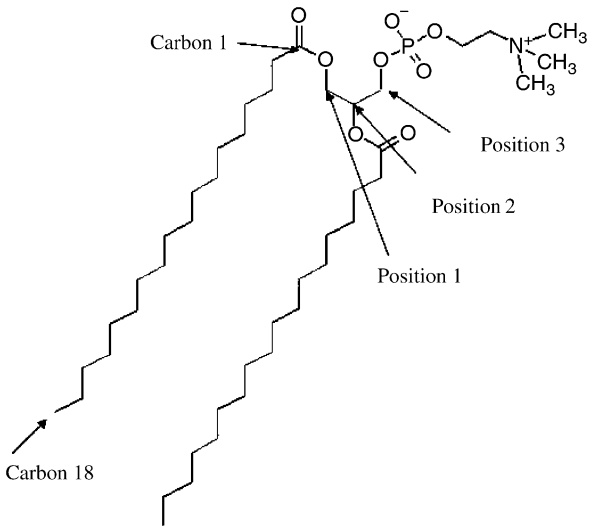

Fig. 1. A schematic of the lipid DSPC, which has two saturated tails of 18 carbons each attached to the glycerol backbone at positions 1 and 2. The phosphatidylcholine headgroup is attached at position 3.

always, the chain attached to the central carbon, number 2, has one double bond in it half way down the chain, while the chain attached to carbon 1 is saturated. A double bond introduces a permanent kink in the chain which makes it difficult to pack efficiently, another recurring theme. The number of carbons in the tails of biological lipids is typically, but not always, around 16 or 18, (i.e., $x = 14$ or 16 above). The length of the tail is often distinguished in the full name of the lipid by an arcane system which, like the jargon of any profession, serves mainly to distinguish those who know it, the insiders, from those who do not, the rest of us. For example, a saturated chain of length 14 is denoted "Myristoyl" (from the tree Myristica Fragrans whose seed is nutmeg, in which, I presume, this lipid is found) while an unsaturated one of the same length is "Myristoleoyl". A saturated chain of length 16 is denoted Palmitoyl, (you can guess where this is found), while an unsaturated one is "Palmitoleoyl". A saturated chain of length 18 is "Stearoyl" while an unsaturated one of the same length is (lest you think you are getting the hang of this) "Oleoyl". So when one sees the moniker "dipalmitoleoylphospatidylcholine," which, once introduced, is invariably abbreviated DPPC, one knows that there are two saturated chains of length 16 with a headgroup of phosphatidylcholine, while DOPE stands for "dioleolyphosphatidylethanolamine," a lipid with two unsaturated chains of length 18 attached to a phosphatidylethanolamine headgroup. The lipid shown schematically in Fig. 1 would be denoted DSPC.

The tails can sample a large number of configurations. They change their shape due to the flexibility around the carbon–carbon bonds. While the most energetically favored state is a chain which goes "straight ahead," (all trans), deviations of 120 degrees clockwise or counterclockwise, (gauche bonds), are not very costly, about $0.8k_BT$, and so will be thermally excited. These thermally excited kinks are in contrast to the "quenched" kink of a double bond.

1.1.2. The origin of self assembly

The hydrogen-bonding network of water is responsible for the self assembly of lipids. If you put anything into water, you disturb this network and reduce its entropy, thus increasing its free energy. If you do not make up for this by some nice attractive interaction, it will cost you free energy to put the object in water. This is the case with the hydrocarbon tails. When you put the headgroups in water, they also break up the hydrogen bonding network. However the favorable interaction of the dipole of the headgroup with the dipoles of water causes the free energy to decrease. Thus the headgroups are hydrophilic while the tails are hydrophobic. As a consequence, the molecules self assemble in water so that the headgroups are exposed, while the tails are sequestered away. There are many possible structures that will accomplish this goal. The most common is the lipid bilayer, with heads out and tails in. Indeed these bilayers serve as the basis for all biological membranes. Various proteins are attached to, or are embedded in, these bilayers which are in a fluid state, (confusingly denoted the liquid crystalline state), so that the diffusion of the proteins is sufficiently rapid that they can go about their jobs. There does exist a lower temperature phase of the lipids, the gel phase, in which the tails are more ordered, (i.e., have fewer gauche bonds) as are the headgroups. Presumably the system is hexatic, that is the headgroups possess long-range orientational order, but no long range positional order. The increased order of the tails permits the lipids to pack more efficiently, with the consequence that it is far more difficult for proteins to make their way through them. In other words, the diffusion constant of the proteins decreases. Because the proteins cannot do their job in a timely fashion, the gel phase is biologically useless. Systems of lipids with two saturated tails of length about 16 or so are in this useless state at body temperature. A replacement of one of the saturated chains of a lipid by an unsaturated one causes a permanent kink in that chain and makes the system difficult to pack. This is reflected in a decrease in the transition temperature from the high temperature liquid crystalline phase to the gel phase. In fact the transition temperature decreases to below that of body temperature, so the system remains in the liquid, biologically useful, phase. It is thought that this is a reason that most biological lipids have one unsaturated, as well as one saturated, chain.

A second structure which lipids can adopt that will keep all parts of their molecules happy is an inverted hexagonal phase, which consists of cylindrical tubes that are stacked in a hexagonal array. The headgroups form the inside of the tubes, and the tails the outside. If there is water in the system, it fills the inner part of the tubes. The inverted hexagonal array is not seen in any biological system of which I am aware, but it is observed frequently in laboratory studies. In fact it is known that some lipids like DOPE (see above) do not form lamellar structures at physiological conditions, but rather form inverted hexagonal phases [1]. This is characteristic of lipids with small headgroups and large tails, as the large tails can sample more configurations

in such a structure than in a lamellar one. I find intriguing the fact that two of the most common lipids found in biological membranes, the phosphatidylethanolamines and phosphatidylserines, would by themselves, prefer to form inverted hexagonal phases. They are trapped in the bilayer by the majority lipids, like the phosphatidylcholines with larger headgroups, which prefer that configuration. Why would Nature want to use in a bilayer lipids that do not want to be there? This is a question to which I shall return.

1.1.3. An apparently simple problem

Given that the lipids form a bilayer, and we know a great deal about them, we should be able to calculate the number of lipids per unit area, i.e., their areal density. This is not as easy as calculating the volume density of liquid Argon, for example, because the lipids have so many internal degrees of freedom. One could attack this problem with molecular dynamics [2]. For the purposes of these lectures, however, I want to follow an alternative approach due to Ben-Shaul et al. [3]. They proceed as follows.

The most difficult part of this problem arises from all of the interactions in the system; the weak, long-range, van der Waals attraction, and the strong, short-range, hard-core repulsion. Ben-Shaul et al. argue that the effect of these interactions is to produce an interior of the bilayer which has a constant, uniform, liquid-like density. Concentrating entirely on the chains for the moment, they replace the Hamiltonian of the system which contains the interactions between chains by one which has no interaction between chains at all. However the partition function is to be calculated subject to the constraint that the density of the bilayer interior is constant. Thus they have converted the original problem into another one, which can be summarized by the equations

$$H = \sum_{\gamma=1}^{n} \sum_{k=1}^{N} h_{\gamma,k}, \tag{1}$$

$$P'_{ex} = \exp[-\beta H]/Q', \tag{2}$$

$$Q' = Tr' \exp[-\beta H], \tag{3}$$

where n is the number of lipid tails, N is the number of segments in each chain, $\beta = 1/k_B T$, and $h_{\gamma,k}$ is the Hamiltonian of a single chain, γ, which now only contains the energy of gauche bonds at segment k. The prime superscript indicates that *only states which contribute a uniform core density are to be considered*. The free energy is obtained from

$$F(T, n, A, V) = Tr' P'_{ex}[H + \beta^{-1} \ln P'_{ex}]. \tag{4}$$

Now this is a difficult problem, but one which we know how to approach. The constraint here is similar to one in a magnetic system in which one wants to sum over states of definite magnetization. Instead of doing this, one changes ensemble in which a magnetic field is fixed as opposed to a magnetization. In such an ensemble one sums over states with any magnetization. The energy of the particular configuration depends upon the magnetic field, and one then chooses the field so that the average magnetization is the desired one. We will follow an analogous procedure.

We define a local volume fraction $\hat{\Phi}(z)$,

$$\hat{\Phi}(z) = \frac{1}{A} \sum_{\gamma=1}^{n} \hat{\phi}_{\gamma}(z), \tag{5}$$

$$\hat{\phi}_{\gamma}(z) = \sum_{k=1}^{N} v_k \delta(z - z_{\gamma,k}), \tag{6}$$

$$\frac{A}{V} \int \mathrm{d}z \hat{\Phi}(z) = 1, \tag{7}$$

where z is the coordinate normal to the bilayer surface, the v_k are the volumes of the kth segment, and the total volume of the system consists only of the sum of its monomeric volumes $V = n \sum v_k$. Under this

incompressibility constraint, the free energy of Eq. (4) becomes a function of only two extensive quantities, $F(T,n,A)$.

Now the probability of a configuration in an external field, $\Pi(z)$, can be written as

$$P_{ex} = \frac{1}{Q} \exp\left[-\beta H - \frac{A}{v_0}\int \mathrm{d}z\, \Pi(z)\hat{\Phi}(z)\right], \tag{8}$$

$$Q = Tr\, \exp\left[-\beta H - \frac{A}{v_0}\int \mathrm{d}z\, \Pi(z)\hat{\Phi}(z)\right], \tag{9}$$

where v_0 is any convenient molecular volume which has only been introduced to make the field $\Pi(z)$ dimensionless. The free energy in this ensemble, which is simply the Legendre transform of $F(T,n,A,\phi)$,

$$G(T,n,\Pi) = F(T,n,A) + \frac{A}{\beta v_0}\int \Pi(z)\,\mathrm{d}z, \tag{10}$$

is given by

$$G = Tr\, P_{ex}\left[H + \frac{A}{\beta v_0}\int \mathrm{d}z\, \Pi(z)\hat{\Phi}(z) + \beta^{-1}\, \ln\, P_{ex}\right]. \tag{11}$$

Because the chains are noninteracting, the probability of a given configuration of all chains is simply the product of the probabilities of each chain to be found in their individual configuration, $P_{ex} = cP_1^n$, where c is an uninteresting constant, and

$$P_1 = \frac{1}{Q_1} \exp\left[-\beta \sum_{k=1}^{N} h_k - \frac{1}{v_0}\int \mathrm{d}z\, \Pi(z)\hat{\phi}(z)\right], \tag{12}$$

$$Q_1 = Tr\, \exp\left[-\beta \sum_{k=1}^{N} h_k - \frac{1}{v_0}\int \mathrm{d}z\, \Pi(z)\hat{\phi}(z)\right], \tag{13}$$

and h_k contains the energy of the gauche bonds of the single chain. The field $\Pi(z)$ is then determined by requiring that the average density be a prescribed, constant, value at *all* z

$$\langle\hat{\Phi}(z)\rangle = \frac{\beta v_0}{A}\frac{\delta G}{\delta \Pi(z)} = 1. \tag{14}$$

One sees from Eq. (13) that Q_1 is the partition function of a single chain in the external field $\Pi(z)$. So the central assumption of Ben-Shaul et al. has reduced the many chain problem to that of calculating the one-chain partition function in an external field. The calculation of this partition function is the central problem in this method, and its difficulty depends on how realistic a description of the chains one takes. Ben-Shaul et al. take Flory's Rotational Isomeric States Model [4] in which each bond between CH_2 groups can take one of three configurations; gauche-plus, gauche-minus, or trans. For m independent bonds, this is only 3^m configurations. However, one also has to specify the *direction* of the chain. This leads to many more configurations. Typically one enumerates on the order of 10^7 chain configurations. Their contribution to the partition function is weighted by the field $\Pi(z)$, and from the partition function one calculates the density. The field $\Pi(z)$ is adjusted until the density is uniform inside the core of the bilayer.

One carries out the calculation of the free energy per chain $g(T,a) \equiv G(T,a)/n$, where $a \equiv A/n$, the area per chain. Because the surface tension $\sigma = \partial g/\partial a$, the minimum of $g(T,a)$ occurs at an area per chain at which the surface tension vanishes, as is expected in experiment. There *is* a minimum because at large areas per chain, the chains must have many gauche bonds in order to fill the space, and these gauche bonds cost energy. At small values of a, the chains must be tightly packed, with the consequence that there are few gauche bonds, and little entropy. The minimum occurs at the optimum trade off of these two effects. The area per chain one obtains from this is a bit large compared to experiment, so Ben-Shaul et al. also include the effect of the repulsive interaction between water and the hydrophobic chains. They take this contribution to the free energy per chain to be $\sigma_0 a$ with σ_0 the usual oil, water interfacial tension. This term shifts the minimum to smaller a and

one finds the minimum to occur at 0.64 nm^2 for a *two-chain* lipid, which is in satisfactory agreement with experiment.

Another nice thing about this calculation is that, because one knows about the equilibrium configuration of the chains, one can calculate their order parameter, which is essentially the angle between CH_2 planes and the bilayer normal. The order parameter can be measured by nuclear magnetic resonance. There is good agreement between theory and experiment.

There is only one catch to this calculation; there is no gel phase. What happened to it? I shall deal with this is the next lecture.

2. Second lecture: Afloat on a sea of phospholipids

The theoretical work in this lecture was inspired by the enormous interest in a relatively new view of the composition of the plasma membrane, the bilayer that surrounds the cell. The canonical view of Singer and Nicholson [5] was that the lipids and cholesterol of this membrane were distributed relatively homogeneously. The newer view [6–10] is that the saturated lipids, like sphingomyelin, and cholesterol, aggregate into regions which float, like rafts, in a sea of the unsaturated lipids, like the phosphatidylcholines. Because the chains of the saturated lipids are relatively more ordered than those of the unsaturated ones, a tendency which is enhanced by the association with cholesterol, the two regions have different areal densities. What got people excited was the observation that various proteins could tell the difference between these regions and would partition preferentially into one or the other. For example, signaling proteins, instead of being distributed uniformly across the plasma membrane, seemed to prefer the raft environment. As a consequence, their local concentration is much larger than it would be if they were uniformly distributed, and this greater local concentration allows them to perform more efficiently. Hence simple *physical* organization leads to organization of *function*.

I must add that this "raft" hypothesis is still controversial. What is very clear however is the result of many experiments in vitro on the ternary system of cholesterol, saturated, and unsaturated lipids [11–14]. Many of them have been carried out by my colleague Sarah Keller and her student Sarah Veatch, and I have been fortunate to be able to discuss these experiments often with them. The clear result is that phase separation occurs commonly in such ternary mixtures. In particular, one sees fairly large regions of composition in which two liquids phase separate. It is extremely tempting to identify this two phase region as one in which rafts would exist; the raft being the more compact fluid, the sea being the less compact one. That the two regions are indeed fluid is easily determined from the shape of the minority regions. They are circular. Were one of them in the gel phase, they would be faceted and irregular. The controversy surrounding the subject of rafts is that nothing so clear as this phase separation has ever been seen in vivo. If such regions do exist, and there is much evidence that they do, they must be very small, and the reason for this is unknown.

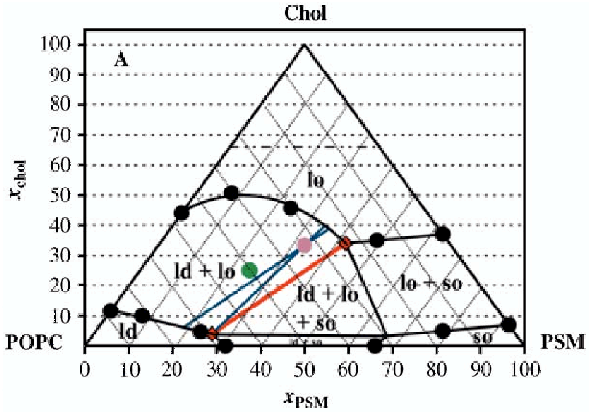

Fig. 2. Sphingomyelin, POPC, cholesterol phase diagram at 23°. The circles are experimental points. Figure from Ref. [11].

The gel phase is also present (in the in vitro systems, for compositions in which the saturated lipid is dominant, and at a temperature below the main chain transition temperature of that lipid.) A phase diagram is shown in Fig. 2 for the system of cholesterol, sphingomyelin (PSM), and palmitoyloleoylphophatidylcholine (POPC) which has one saturated chain of 16 carbons and an unsaturated one of 18 carbons. In that diagram, the cholesterol-rich liquid phase, in which the mostly saturated lipids have relatively well-ordered chains is denoted "lo" for liquid-ordered, the cholesterol-poor liquid phase, in which the mostly unsaturated lipids have less well-ordered chains, is denoted "ld" for liquid-disordered, and the gel phase is denoted "so" for solid-ordered, notation that originates in an influential theoretical paper [15]. There is a fairly large three-phase triangle.

I originally thought that understanding the gel phase might be the key to understanding rafts. I reasoned as follows. I know that the main-chain transition is *first* order. That means that all of the *first* derivatives of the free energy with respect to intensive variables, are discontinuous at the transition. In particular, the densities, which are first derivatives of the free energy with respect to chemical potentials, will be discontinuous. Thus the binary system of unsaturated lipid and saturated lipid will show coexistence between an unsaturated lipid-rich liquid, (the "ld"), and the gel. Similarly the binary system of cholesterol and saturated lipid will also show coexistence between a cholesterol-rich liquid phase, (the "lo") and the gel phase. I thought it not unlikely that, in the ternary system, these two liquids would have a region of coexistence because the well-ordered tails of the lipids in the liquid-ordered phase would not pack well with the more disordered tails in the liquid-disordered phase. Thus understanding the order in the tails, as exemplified by the gel phase, might be key.

This raises the question as to why the calculation of Ben-Shaul et al. misses this phase? The answer is that the order in the bilayer core is described by these authors entirely in terms of the local density; i.e., they require only that the local density be constant. Now it is conceivable that chains obeying this constraint might not be particularly well ordered, for the constraint says nothing about the order of the local bonds between carbons which, one would expect, should be relatively parallel if only so that the chains do not intersect, which would be energetically costly. Thus it seems that one needs to describe not only the local density of carbon atoms, but the local density of bonds between them. The local orientation of the chain is conveniently specified by the normal to the plane determined by the kth CH_2 group,

$$\mathbf{u}_{\sigma,k} = \frac{\mathbf{r}_{k-1} - \mathbf{r}_{k+1}}{|\mathbf{r}_{k-1} - \mathbf{r}_{k+1}|}, \quad k = 1 \ldots N-1. \tag{15}$$

Next one defines a function, $\hat{\xi}_\sigma(z)$, which tells you how well these local bonds are oriented with respect to the bilayer normal $\mathbf{c}$,

$$\hat{\xi}_\sigma(z) = \sum_{k=1}^{N-1} v_\sigma(k)\delta(z - z_k) g(\mathbf{u}_\sigma \cdot \mathbf{c}), \tag{16}$$

where

$$g(\mathbf{u}_\sigma \cdot \mathbf{c}) \equiv (m + \tfrac{1}{2})(\mathbf{u}_\sigma \cdot \mathbf{c})^{2m}. \tag{17}$$

For large m, $g \approx m \exp(-m\theta^2)$ where θ is the angle between the two unit vectors. Matching lipid parameters, one finds $m = 18$ is reasonable. Note that $g(\mathbf{u}_\sigma \cdot \mathbf{c})$ is unity if the bond vector $\mathbf{u}$ is aligned with the bilayer, and falls exponentially with the angle between the two vectors.

To express the fact that it is energetically favorable for bonds which are in the same local region to be aligned with one another, and with the bilayer normal, one adds a simple interaction

$$V(\mathbf{u}, \mathbf{u}') = -(J/v_0) g(\mathbf{u} \cdot \mathbf{c}) g(\mathbf{u}' \cdot \mathbf{c}). \tag{18}$$

Note that this interaction is not rotationally invariant because the environment is not rotationally invariant; the bilayer is given, so that its normal specifies a preferred direction.

One can now carry out the same sort of program that we did before, and this was done by Richard Elliott [16]. The difference is that one now finds a nice, first-order, main-chain transition in the system of saturated lipids. We set the value of the interaction strength, J, so that the transition temperature, T^*, for the saturated chains of model DPPC agreed with experiment, 42 °C. We then repeated this calculation for a system of a mono-unsaturated lipid, DOPC. We kept the same interaction strength, because the interaction is between

bonds in a hydrocarbon chain, irrespective of whether that chain does or does not have a double bond somewhere in it. The only difference in the calculation is that one uses the ensemble of configurations of a chain with a single double bond in it. As noted earlier, one knows that the presence of this bond makes packing more difficult and should lower the transition temperature dramatically. To our great satisfaction, we found that this is precisely what the calculation tells us; the transition temperature is now less than 0 °C, in agreement with experiment. Mixtures of these two lipids are easily handled and, at the main-chain transition of DPPC, a phase separation is encountered between a DPPC-rich gel and a DOPC-rich fluid. This is what we expect as a consequence of the first-order main chain transition.

We have now brought two of the major players onto the stage. It remains only (only!), to introduce the third; cholesterol. In order to fulfill the constraint of constant density within the bilayer, we need to know where all the atoms in cholesterol are, which we do. We also have to keep track of its configurations, just as for the lipids. This is not as difficult because much of the cholesterol molecule is rigid, so if one know where two of the atoms are, one knows where they all are. There is a small hydrocarbon chain at one end of the molecule, and this is treated like the lipid chains. As there are now chains and cholesterol, there are now three interactions: between lipid chains, as before; between lipid chains and cholesterol; and between cholesterol and cholesterol. All interactions are taken to be of the form of Eq. (18) with strengths J_{ll}, J_{lc}, and J_{cc}. As the first strength is set by the main chain transition temperature of DPPC, we have two interaction strengths at our disposal.

We first asked what would the system do if the additional two interactions, those involving cholesterol, were zero; that is, the cholesterol would only affect the system due to its volume through the packing constraint. We found the phase diagrams of Fig. 3. One sees that the gel separates from the disordered fluid and the cholesterol rich fluid, but there is no liquid–liquid phase separation anywhere. Recall, that the region of liquid–liquid phase separation is where the "rafts" would be.

Next, to test my view that the existence of liquid–liquid coexistence in the ternary system was due to the fact that a relatively well-ordered cholesterol-rich liquid would want to separate from a more disordered cholesterol-poor liquid, we turned on the lipid-cholesterol interaction so that the cholesterol-rich liquid would be relatively well-ordered in contrast to the disordered fluid. I believed that these two liquids would phase separate. To my dismay, they did not. The major effect of an attractive interaction between cholesterol and lipid is that the gel phase becomes swollen with cholesterol, something which is not observed. So my whole thinking about this problem was wrong, and had to change. It did. As a result, we looked at the effect of the attractive interaction between cholesterols. This had the (not unexpected) effect to cause a phase separation between cholesterol and lipids. In particular, in the binary saturated lipid cholesterol system, there was a transition to a cholesterol-rich, more-ordered liquid, and a cholesterol poor less-ordered liquid. See Fig. 4. Such a separation had been observed long ago by Vist and Davis [18]. When one adds the unsaturated lipid, this region of liquid–liquid coexistence simply extends into the ternary diagram. Again, this liquid–liquid region is the region of rafts. The interested reader can find further details in the paper where the above was described [17].

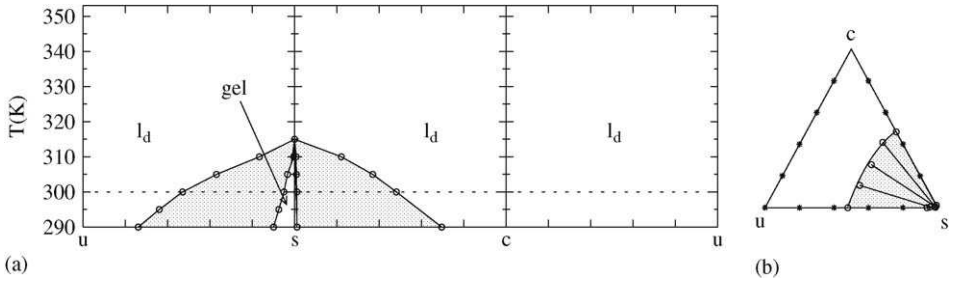

Fig. 3. Calculated phase diagrams of the three binary mixtures of cholesterol (c), saturated (s), and unsaturated (u) lipids in temperature-composition space for $J_{ll}(m+1/2)^2/k_BT^* = 1.44$ and $J_{lc} = J_{cc} = 0.0$. These binary diagrams form the sides of the Gibbs prism, a cut through which at 300 K produces the Gibbs triangle shown in Fig. 2(b). Regions of two-phase coexistence are shaded, and some tie lines are shown. Figure from Ref. [17].

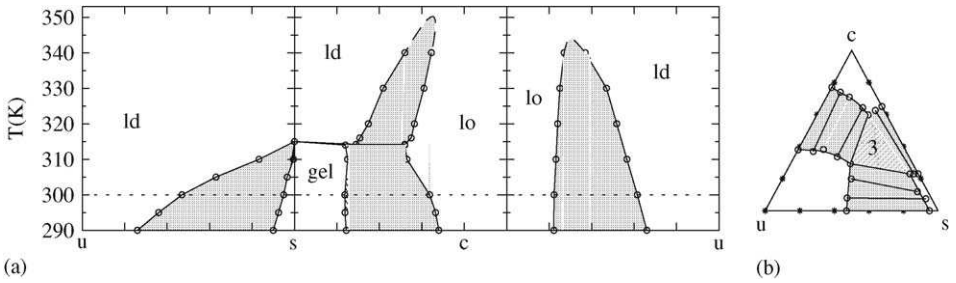

Fig. 4. a. Binary phase diagrams for $J_{lc} = 0.78J_{ll}$ and $J_{cc} = 0.73J_{ll}$, and J_{ll} as in Fig. 3. The saturated lipid-cholesterol mixture has a triple point very near the main-chain transition temperature, so that the gel, l_d coexistence region is very narrow. Dashed lines are extrapolations. The ternary mixture at $T = 300\,\mathrm{K}$ is shown in b. Figure from Ref. [17].

So the physics behind the liquid–liquid coexistence turns out to be exceedingly simple. It is due to the preference of the cholesterol and lipids to phase separate, which gives two liquids, one cholesterol-rich, the other cholesterol-poor. Due to the tendency of the rigid cholesterol molecule to order the lipid chains around it, the cholesterol-rich liquid is the "ordered liquid," while the cholesterol-poor liquid is the "disordered liquid". The gel phase, which occurs at lower temperatures, causes there to be additional regions of coexistence between gel and liquid-ordered, and gel and liquid-disordered, and a three-phase triangle. But these merely take up valuable real estate in the three phase triangle. The gel phase has nothing to do with the existence of the liquid–liquid coexistence region. Our results for the ternary phase diagram at $T = 300\,\mathrm{K}$ are shown in Fig. 4. It looks very much like the experimental one of Fig. 2. So I think that we now understand the "in vitro" experiments. Understanding those "in vivo" may be a little more difficult.

3. Third lecture: Delivering drugs

The problem posed here is how to get a drug to a target within a cell. One method that looked promising was to make use of a virus, as they have evolved to get into a cell very efficiently. An example is the influenza virus, a single strand of RNA enveloped in a small vesicle composed of lipid bilayer. The cell takes it in, and surrounds it with an vesicle of its own called an endosome. If the RNA does not get out of the endosome in good time, it will be destroyed. To get out of the endosome, the virus's own vesicle fuses with it, a process which is triggered by the natural decrease in the pH within an endosome over its lifetime. The pH decreases from the normal 7.3 to about 5, which is quite acidic.

The basic idea was to alter the virus so that, instead of instructing the cell to reproduce the virus, it would instruct the cell to make a drug of choice. There are dangers in using a virus, however. It may become virulent, or trigger an immune reaction, as well as other possibilities. As a consequence, there is a very active line of research to try to make non-viral drug delivery systems, ones which mimic the viral one, but which are benign. It is not difficult to encapsulate a drug in a vesicle, have the vesicle taken up by the cell, and be encapsulated within an endosome. However, it is difficult to get the drug out of the endosome before the drug is destroyed. Taking a cue from the natural process, one asked whether it were possible to design a vesicle to encapsulate the drug which would be sensitive to the changing pH of the endosome, and to release it as the pH changed. It was hoped that in the process, the drug would also escape the endosome.

One can do this. We have already encountered the idea that architecture matters; that lipids with headgroups and tails of comparable volumes tend to make bilayers, while those with small headgroups and large tails tend to make inverted hexagonal phases. Phosphatidylserine, (PS), is a lipid whose architecture can effectively be changed by changing pH. At normal pH, its COOH group is ionized. The resulting negative charge attracts positive counterions, like $H_7^+O_3$ and $H_5^+O_2$, with the consequence that its headgroup is effectively larger, and the lipid makes bilayers. Thus a vesicle can be made from it. If the pH is reduced to 3.6, only half of the COOH is ionized. Below this pH, the headgroup is essentially neutral. Without the additional waters, the headgroup is sufficiently small that the lipid no longer makes bilayers, but makes an inverted hexagonal phase. Therefore, if one made a vesicle of PS, it would fall apart at a pH of about 3.6 and release its

cargo. This is fine, but a pH of 3.6 is of little use biologically. One would like the vesicle to fall apart at a value of about 5, preferably at a value that can be tuned. Can this be done?

A clever answer was provided by Hafez et al. [19]. They suggested that one combine an ionizable anionic lipid with a permanently ionized cationic lipid. For the ionizable ionic lipid, they chose cholesteryl hemisuccinate (CHEMS), instead of PS, and for the permanently ionized cationic lipid chose N,N-dioleoyl-N,N-dimethylammonium chloride, or DODAC. A bilayer made of CHEMS is unstable for a pH less than 4.2 for the same reason that the PS bilayer is unstable at pH of 3.6. So let us begin with a CHEMS bilayer at some pH just slightly greater than 4.2. The positive counterions just stabilize the bilayer. What is the effect of adding a small amount of permanently charged positive lipid? Well, fewer positive counter ions are now needed for neutrality. But with fewer positive counterions, the bilayer will fall apart. So in order to make it marginally stable again, one will have to attract more counterions by ionizing more CHEMS; that is, one will have to increase the pH. Thus the pH at which the bilayer falls apart increases with increasing concentration of permanently ionized cationic lipid. The vesicle which falls apart at a tunable pH is therefore achievable.

To understand this process better, Xiao-jun Li and I decided to investigate it theoretically using a model we had proposed earlier [20]. In it, the two-tail lipids are treated as a triblock copolymer of the form BAB. The B tails are completely flexible, and of course take up volume. The A headgroup has no entropy whatsoever, but does have a volume. The system is embedded in a solvent of A monomers with their own volume. The advantage of using block copolymers over the model used in the first two lectures is simple. As noted earlier, the heart of the method used in the first two lectures is to calculate the partition function of a single lipid in a given external field. Using the Flory model that we did to describe the relatively short-chain tails, this calculation was very difficult. We had to generate explicitly on the order of 10 million configurations of the tails. On the other hand, if one models the tails as completely flexible, the partition function can be calculated simply by solving a modified diffusion equation for a particle in an external field [21,22].

The only concern we had about the model was whether the completely flexible chains simply had too much entropy. To check this, we calculated [20] the phase diagram of our model lipid with volume fractions of head and tail appropriate to that of DOPE in water. The unknowns in the calculation are the local volume fraction of headgroups, $\phi_h(\mathbf{r})$, the local volume fraction of tails, $\phi_t(\mathbf{r})$, and the local volume fraction of water, $\phi_w(\mathbf{r})$. We took but a single interaction, a local one between A and B entities, that is, between tails and headgroups, and between tails and water. To model the hard-core interactions, we imposed an incompressibility constraint

$$\phi_t(\mathbf{r}) + \phi_h(\mathbf{r}) + \phi_w(\mathbf{r}) = 1. \tag{19}$$

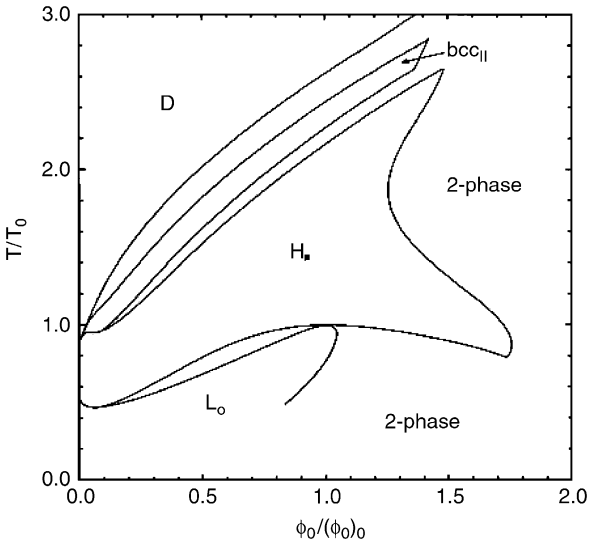

Fig. 5. Phase diagram of a neutral lipid which models DOPE in water as a function of temperature, T/T_0 and solvent fraction, $\phi_s/(\phi_s)_0$, where T_0 and ϕ_0 are the temperature and volume fraction of solvent at the azeotrope. Figure from Ref. [20].

The resulting phase diagram, shown in Fig. 5, is in rather good agreement with experiment [23,24]. They both show the progression from lamellar to hexagonal to body-centered-cubic with increased temperature, an effect due to the entropy of the tails. More interestingly, they both show an azeotrope at which the lamellar phase undergoes a first-order transition to an inverted hexagonal phase with no change in water content. This agreement allayed any fears that the tails contributed too much entropy.

The system of two charged lipids and solvent is certainly quite complicated, as it is characterized by *eight* unknown functions; the local volume fraction of the headgroups of the two anionic lipids, $\phi_h^{(1)}(\mathbf{r})$ and $\phi_h^{(2)}(\mathbf{r})$, the volume fraction of the tails of these two lipids, $\phi_t^{(1)}(\mathbf{r})$ and $\phi_2^{(2)}(\mathbf{r})$, the volume fraction of the solvent, $\phi_s(\mathbf{r})$, and of the counterions, $\phi_c(\mathbf{r})$, the local *charge* density of the headgroup of the anionic lipid, $eP_h^{(1)}(\mathbf{r})$ and of the cationic lipid, $eP_h^{(2)}(\mathbf{r})$. The interactions among the elements are of two kinds. Just as in the neutral system, there are the repulsive local interactions between tail segments and heads, and tail segments and solvent. In addition, there are now Coulomb interactions between all charges. Finally there is the incompressibility constraint. Within self-consistent field theory, the problem quickly reduces to solving four self-consistent equations, one of which is the Poisson–Boltzmann equation.

The results are gratifying [25]. Fig. 6 shows our results for the fractional concentration of the ionizable anionic lipid, Θ, as a function of pH with respect to the pK of the anionic lipid headgroup. The pK is defined as that value of the pH at which one half of the headgroup is ionized. We have taken the pK of CHEMS to be 5.5, which is reasonable. The solid lines show the coexistence between lamellar and inverted hexagonal phases we obtain, and the dots are the experimental results [19]. When there is no DODAC in the system, the transition occurs at some value of the pH which is quite far below the pK of 5.8. However as one adds the permanently ionized cationic lipid, so that Θ decreases, the transition now occurs at larger pH, so the pH of the transition, the place where the vesicle will fall apart, is tunable as advertised. One also sees that there is a nice regime where the pH of the transition is extremely sensitive to the concentration of the cationic lipid, a desirable feature. The dotted line in the figure is a criterion of Hafez et al. which derives from an understanding of the problem which is different than ours, and is not of interest here.

However, from our own understanding it was clear that the desirable feature of tunability was not limited to the use of the combination of ionizable, anionic, lipid and permanently charged cationic lipid. One could also use an ionizable, anionic lipid, and a *neutral* lipid, like PE, which prefers to make inverted hexagonal phases. In order to stabilize a lamellar phase, one must add the ionizable anionic lipid. When there is little of the ionizable lipid in the system, it must be fully charged (producing a large effective head-group) to stabilize the bilayer vesicle. Thus the pH must be very large. As more of it is added, the headgroups need not be so fully

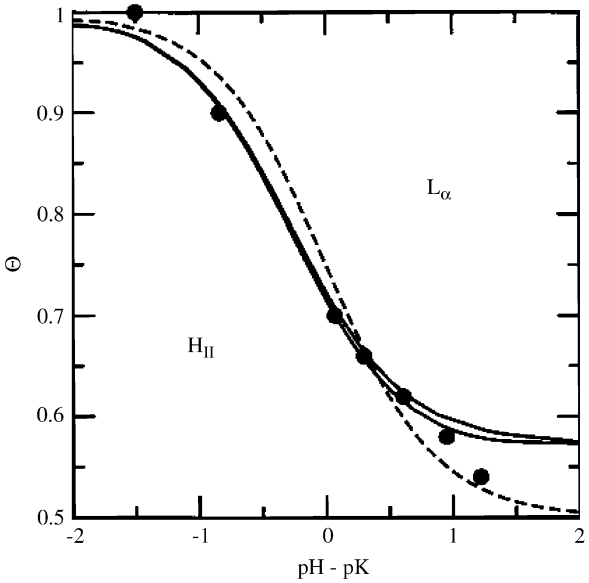

Fig. 6. Phase diagram at a fixed temperature of a mixture of ionizable, anionic lipid, and fully ionized cationic lipid. Figure from Ref. [25].

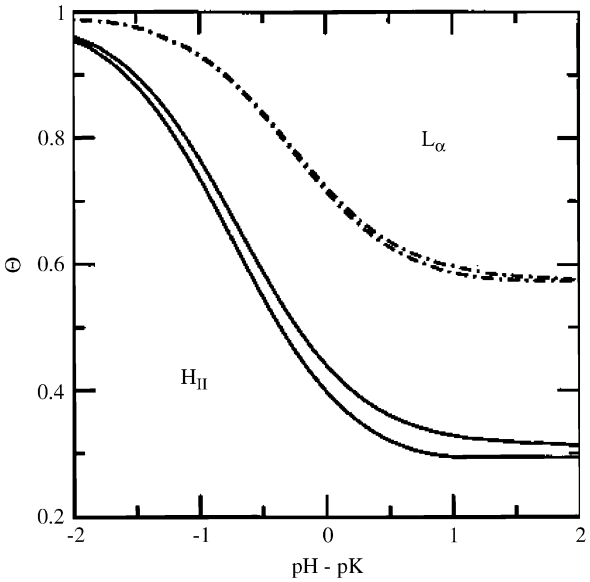

Fig. 7. Phase diagram at a fixed temperature of a mixture of ionizable, anionic lipid, and neutral lipid. Solid lines show the coexistence from the calculation. For comparison, the dashed lines show the calculated coexistence for the ionizable anionic and fully ionized cationic lipid system shown previously in Fig. 6. Figure from Ref. [25].

charged, so the pH of the transition will decrease. This understanding was borne out by our results shown in Fig. 7. Again the relative concentration of ionizable lipid, Θ, is shown as a function of pH–pK. The phase boundary in this system with a neutral lipid is similar in behavior to that of the system with a permanently charged lipid, the results of which are reproduced in dotted lines. That one could use a neutral and a charged lipid holds out the prospect that one could make a tunable vesicle simply from naturally occurring PS and PE lipids.

One interesting process involved in drug delivery, or in viral infection, which I would like to address is just how the vesicle which encloses the drug, or the single-stranded RNA, fuses with the endosome that surrounds it. This is one of the many problems subsumed under the more general problem of membrane fusion, which will be the topic of my final lecture.

4. Fourth lecture: Membrane fusion

The fusion of biological membranes is an enormously important process for several reasons. Many molecules that the cell needs are made within the cell itself. In order to send these molecules to the locations at which they are needed, they are often enclosed in lipid vesicles. Once they arrive, these vesicles must fuse with other vesicles in order to relay their cargo to the new location. This process, which goes under the rubric of "trafficking," has attracted for many years the attention of biologists who want to know how the cargo vesicle recognizes the target vesicle. Another process of great importance is endocytosis, responsible for getting something made in the cell, serotonin for example, to the outside, like a neural synapse. The serotonin is enclosed in a lipid vesicle which makes its way to the plasma membrane which encases the cell. The vesicle must then fuse with the membrane in order to release its cargo to the outside. A third example is the viral entry which I discussed last lecture.

For all its importance, the physics of membrane fusion is not well understood at all. In fact, what I see as the central conundrum which fusion presents seems, with notable exceptions [26], not to have been addressed explicitly. That conundrum is the following. In order for any vesicle to be useful, it must be relatively stable. In particular, its enclosing membrane must be stable to the occurrence of long-lived holes which are thermally activated. Yet in order to undergo fusion, just such long-lived holes must occur at some point along the fusion

pathway. It would seem that vesicles could *either* be stable, *or* they could undergo fusion, but not both. How they actually manage to exhibit these two conflicting properties is the conundrum. Because of recent work on this problem, [27,28], I believe the resolution of this puzzle can be understood.

I shall briefly review the situation. We begin with two membranes, each consisting of two layers of amphiphiles, or lipids. In general the head groups of the lipids like to be surrounded by water. To bring the membranes sufficiently close together so that fusion can occur, the interposed water must be removed, at least in some region between the membranes. To remove this water takes energy which, presumably, is provided in vivo, by fusion proteins. Due to the loss of water between membranes, the free energy per unit area, or surface tension, of the membranes increases. One possible response of the system to this increase is to undergo fusion because this process, by making holes in the membranes, decreases the membrane area and thus the free energy. The canonical way this has been thought to occur (see [26] and references therein) was first suggested by Kozlov and Markin [29], and is illustrated in Fig. 8.

In panel (a) we see two bilayers under zero tension, They are composed of amphiphiles, block copolymers in this case, which contain a fraction $f = 0.35$ of the hydrophilic component. Only the majority component is shown at each point: solvent segments are white, hydrophilic and hydrophobic segments of the amphiphile are dark and light correspondingly. Distances are measured in units of the polymer radius of gyration, R_g, which is the same for both the amphiphiles and for the homopolymer solvent. In (b), tails of some amphiphiles in a small region have turned over, attempting to form an axially-symmetric "stalk". This panel shows the transition state to the formation of the stalk, and panel (c) shows the metastable stalk itself. After the stalk forms, the layers pinch down and expand, pass through a second intermediate, shown in (d), and arrive at a hemifusion diaphragm, (e). A hole then forms in this diaphragm, which completes formation of the fusion pore. Note that the conundrum is not addressed explicitly by this scenario. However, one can observe that this mechanism requires a hole to form only in the *one* hemifusion diaphragm rather than in the *two* bilayers separately.

Sometime ago, Marcus Müller, Kirill Katsov, and I decided to watch, via Monte Carlo simulation, the fusion process unfold in a system of bilayers formed by block copolymers in homopolymer solvent [30]. Our choice of this system of non-biological amphiphiles was motivated by the fact that we had experience in simulating such amphiphilic copolymers, and our belief, as physicists, that the fusion process was probably universal. The time and energy scales would vary from system to system, but not the pathway of the process itself. Furthermore vesicles of block copolymer form a novel family which is currently being investigated for its technological possibilities [31]. Details of the simulation can be found in [30,32], but the results can be summarized as follows. Upon putting the bilayers under tension and in close apposition, we did see the formation of an axially symmetric stalk. We expected to see the stalk expand radially, but it did not. Instead, it expanded asymmetrically, forming a worm-like structure which moved about. We also observed that once the stalk formed, the rate of hole formation in either bilayer rose dramatically. This is shown in Fig. 9 where, in the lower panel, the rate of hole formation in each bilayer, one in black, the other in gray, is seen to rise dramatically after about 200 time steps when we know, independently, that a stalk had formed. The rate of hole formation in a *single* bilayer is shown in the upper panel for comparison.

Furthermore, we could determine that the stalk and the newly-created holes were correlated; that is, for the most part, the holes formed very near to the stalk. Once a hole formed in one bilayer next to the stalk, the latter, which we had observed to be quite mobile, proceeded to walk around the hole, thereby forming something like a hemifusion diaphragm. After a second hole pierced this diaphragm, the fusion pore was complete. In a slightly different scenario, we saw a hole form in one bilayer, and the stalk begin to walk around it. Before it completely surrounded the first hole, a second one appeared in the other bilayer near the stalk. The stalk then had to corral the two holes, walking around them both, to complete the fusion pore. The fusion intermediate in this latter scenario is shown in Fig. 10. One sees in (a) the two aligned holes. To the right in the figure, one sees that the holes have occurred in the two bilayers separately, while to the left one sees the stalk moving around the perimeters of the holes and sewing them together to form the fusion pore. The analogous picture in the former scenario differs in that there is a hole only in one bilayer, while the other is still intact. The stalk would be seen surrounding the one hole to form the hemifusion diaphragm.

It is clear that in the mechanism we saw, the formation of a fusion pore is closely correlated, in space and time, with hole creation. This correlation is seen in Fig. 11; the formation of pores closely follows in time the

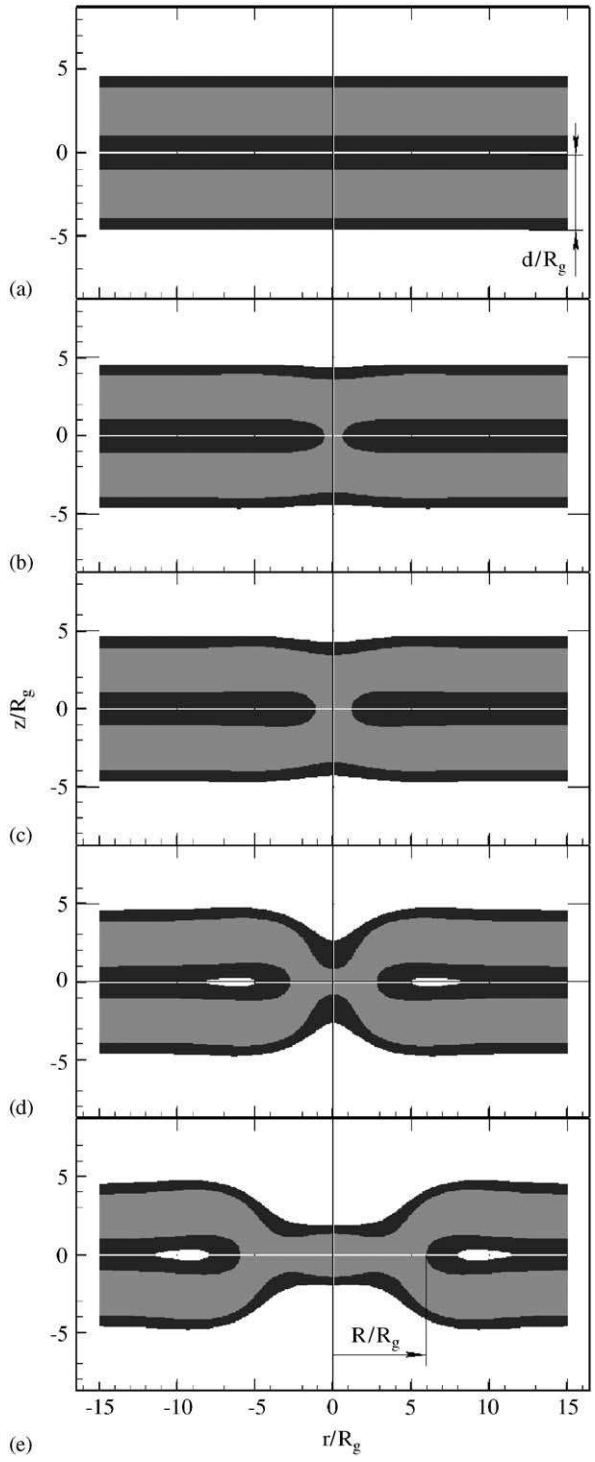

Fig. 8. Density profiles of structures from bilayers in apposition, (a), passing through a metastable stalk (c), to a hemifusion diaphragm (e). Figures are shown in the r, z plane of cylindrical coordinates. Figure from Ref. [27].

onset of hole formation triggered somehow by stalk formation. There is a clear experimental differentiation between this new mechanism, and the standard hemifusion mechanism discussed earlier. This consequence, transient leakage, can be understood from Fig. 12 which shows that for a certain period of time, there is a hole

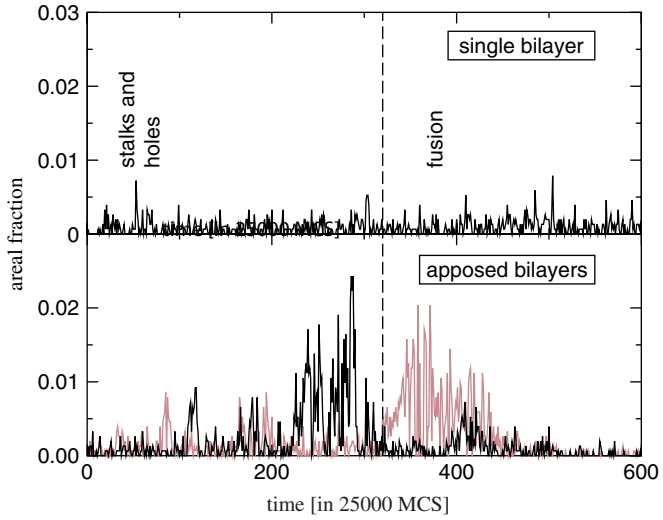

Fig. 9. Area of holes vs. time in the system of two apposed bilayers, bottom, and in an isolated bilayer, top. Figure from Ref. [32].

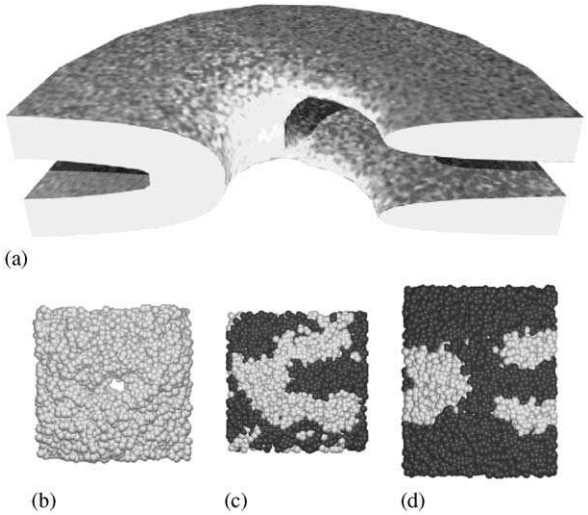

Fig. 10. The fusion intermediate in one of the scenarios of the new fusion mechanism. (a) Schematic sketch of the intermediate. Only hydrophobic portions are shown. (b) Top view of a fusion pore through two membranes. Only hydrophobic portions are shown. (c) Top view of the layer between the two membranes. Hydrophilic segments are dark gray, hydrophobic segments are light gray. (d) Side view of the snapshot. Figure from Ref. [30].

from at least one of the vesicles to the outside during the fusion process. How much leakage there is depends on what molecule one is observing, as each will have its own characteristic time to diffuse through the hole. If this time is significantly greater than the time for the stalk to surround the hole and seal it up, there will be little, if any, observable leakage. However if the time to diffuse to the hole is much less than the sealing time, there will be. Just such leakage, correlated with fusion in the manner of Fig. 11, was recently observed in an elegant experiment [33].

How do we understand the behavior we have seen in our model, and by others [34] in a more simplified model? We had an idea as to what was going on, and to verify it, we embarked on a series of self-consistent field calculations [27,28] on the same system as had been simulated, from which various free energies could be calculated explicitly.

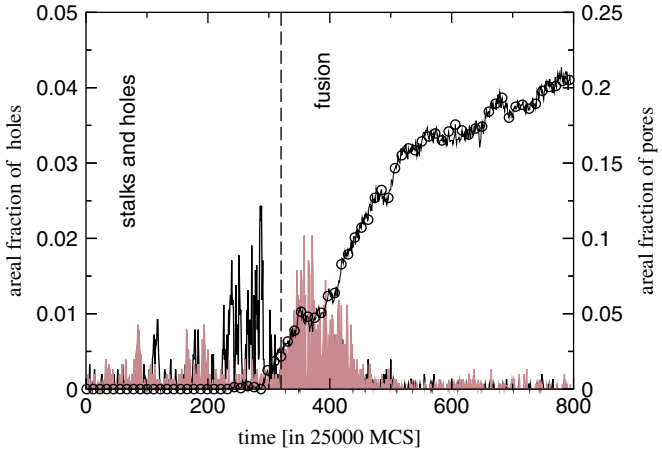

Fig. 11. Area of pore (symbols) and of holes (lines) for one simulation run, the same as shown in Fig. 9. Note the different scale for pore and hole areas. Figure from Ref. [32].

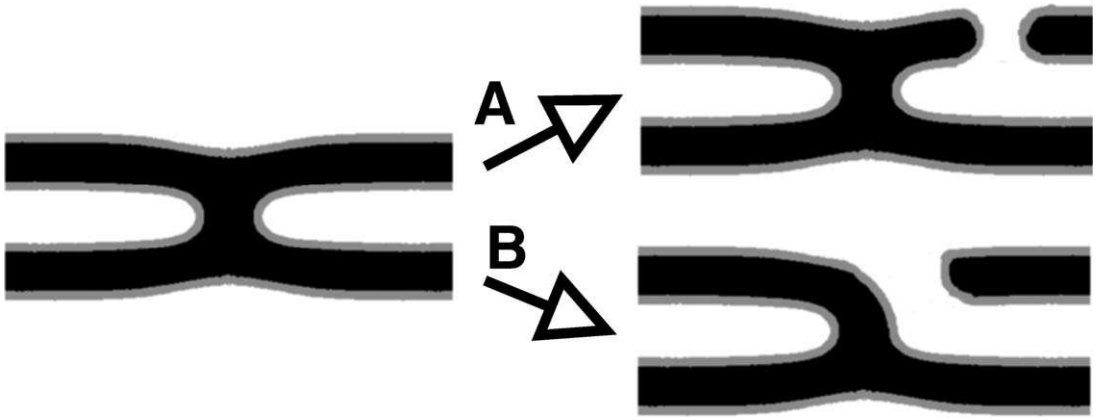

Fig. 12. A schematic diagram which makes plausible that the line tension of a hole which forms near a stalk, as in path B, is less than if it forms far from a stalk, as in A.

We began with the standard pathway to fusion; a stalk which expands radially to form a hemifusion diaphragm which is then pierced by a hole to form a pore. Our results for the stalk to hemifusion diaphragm part of this path is shown in Fig. 13. The upper panel shows the results for the free energy, in units of k_bT, of the stalk as it expands into a hemifusion diaphragm, as shown in Fig. 8. The radius of this axial symmetric object is R, and is measured in units of the radius of gyration, R_g of the polymer. The bilayer is under zero tension. Curves are shown for bilayers comprised of amphiphiles of different architecture, f, the fraction of hydrophilic segments in the amphiphile. An $f = 0.5$ corresponds to an amphiphile with equal volume fraction of hydrophilic and hydrophobic parts, one which certainly will make lamellae. As f decreases, the amphiphiles, though still lamellar forming, approach a stability limit at which inverted hexagonal phases are most stable. The stalk forms at an r/R_g between 1 and 2, as shown in the inset. One sees that its energy of formation is low. One also sees that there is a local minimum for this stalk if the architecture is near $f \approx 0.35$. If the amphiphiles have too large an f, that is, are too lamellar forming, this local minimum disappears and the stalk would not be metastable. On the other hand, if the amphiphiles are characterized by too small an f, so that they are too inverted-hexagonal forming, then the stalk's free energy is negative, less than that of the unperturbed bilayers, with the consequence that an inverted hexagonal phase will be stable, and the bilayer unstable. Clearly for fusion to be initiated by a stalk, the architecture has to be adjusted within a relatively narrow range.

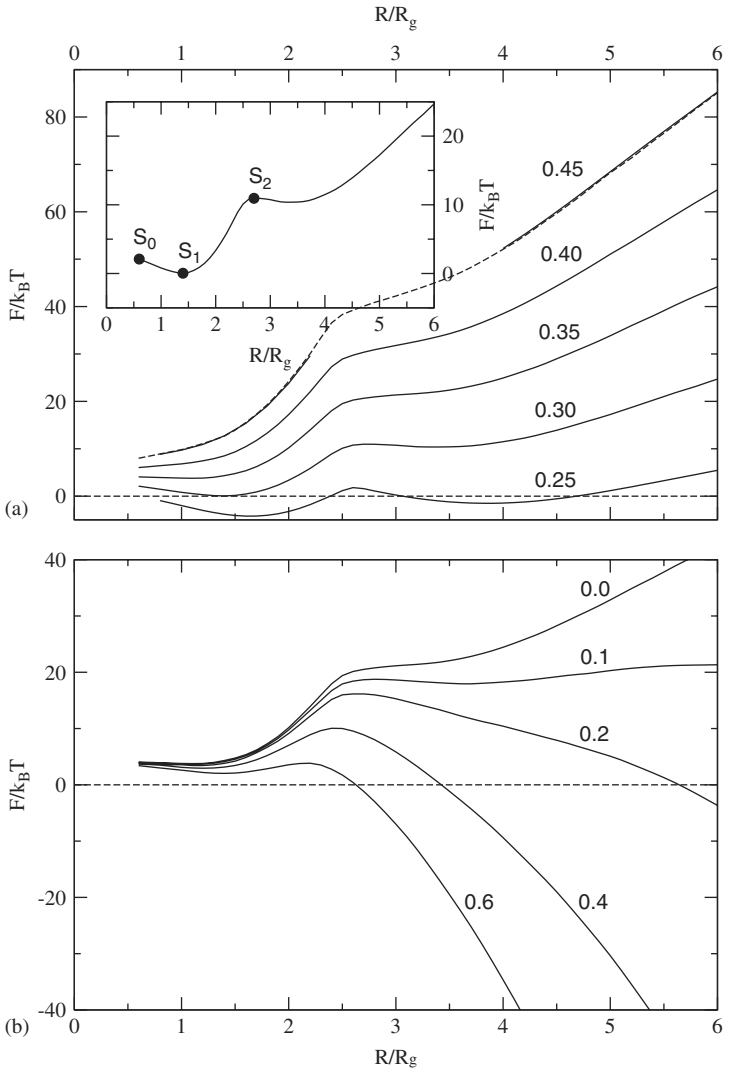

Fig. 13. (a) The free energy, F, of the stalk-like structure connecting bilayers of fixed tension, zero, is shown for several different values of the amphiphile's hydrophilic fraction f. In the inset we identify the metastable stalk, S_1, the transition state, S_0, between the system with no stalk at all and with this metastable stalk, and the transition state, S_2, between the metastable stalk and a hemifusion diaphragm. The architectural parameter is $f = 0.30$ for this inset. No stable stalk solutions were found for $f = 0.45$ in the region shown with dashed lines. They were unstable to pore formation. (b) The free energy of the expanding stalk-like structure connecting bilayers of amphiphiles with fixed architectural parameter $f = 0.35$ is shown for several different bilayer tensions. These tensions, $\gamma/\gamma_{\rm int}$, are shown next to each curve. Figure from Ref. [27].

As the stalk expands into a hemifusion diaphragm, the free energy increases. If the bilayer is under zero tension, the fact that the hemifusion diaphragm has eliminated bilayer area does not decrease the free energy which continues to rise due to the increased circumference of the diaphragm which costs free energy $2\pi R\lambda_{hd}$ due to the line tension, λ_{hd} of this circumference. However if the bilayer is placed under tension, γ, the free energy eventually decreases like $-\gamma\pi R^2$ and the free energy displays a maximum, as seen in the lower panel of Fig. 13. We found that the hole forms when the diaphragm has expanded beyond this barrier, so that this barrier to hemifusion expansion *is* the largest barrier along this path to fusion. One sees from this figure that the barrier to fusion along this pathway decreases with increasing tension, as one would expect.

The architectures for which successful fusion is possible, as discussed above for membranes under zero tension, depends somewhat on tension, and is shown in Fig. 14. This architectural constraint on successful

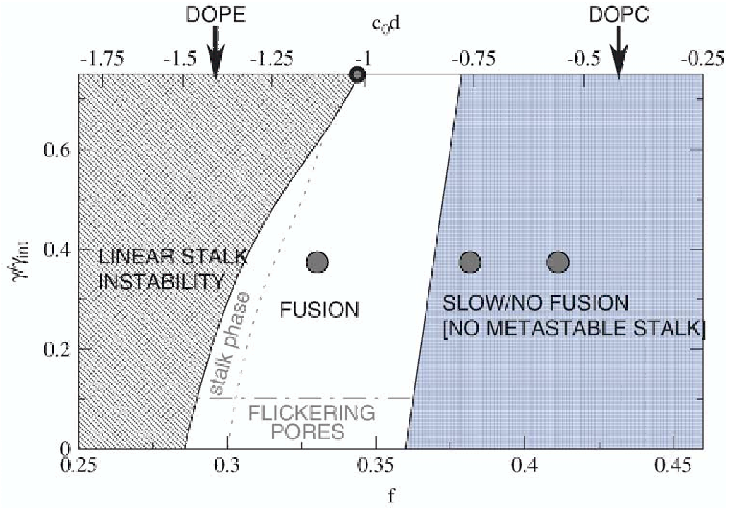

Fig. 14. A "phase diagram" of the hemifusion process in the hydrophilic fraction-tension, (f,γ), plane. Circles show points at which previous, independent, simulations were performed by us. Successful fusion can occur within the unshaded region. As the tension, γ, decreases to zero, the barrier to expansion of the pore increases without limit as does the time for fusion. As the right-hand boundary is approached, the stalk loses its metastability causing fusion to be extremely slow. As the left-hand boundary is approached, the boundaries to fusion are reduced, as is the time for fusion, but the process is eventually pre-empted due to the stability either of radial stalks, forming the stalk phase, or linear stalks, forming the inverted hexagonal phase. Figure from Ref. [27].

fusion applies to *any* fusion mechanism which begins with a stalk. In particular it applies to the alternate mechanism proposed above which also begins with a stalk.

To calculate the fusion barriers in the new mechanism is more difficult than to calculate them in the old. This is because the intermediates in the new mechanism do not possess axial symmetry, a symmetry which can be exploited to reduce the difficulty of the calculation. Nonetheless Kirill Katsov was able to surmount these difficulties and did obtain the barriers in the new mechanism. The barriers in the new and old pathways are shown in Fig. 15(a) and (b), respectively. One notes that the free energy barriers in the new mechanism are lower than in the old, though not by a large amount. The new mechanism becomes increasingly favorable as the amphiphiles making up the bilayer become more hexagonal-forming, that is, as f decreases.

Why should the new mechanism be more favorable, free energetically, than the old? We observe that in order for this new mechanism to be favorable, two conditions must be met. The first is that it must not cost too much free energy for the stalk to elongate in a worm-like fashion, in the manner that it does before the hole appears. That this can be the case is clear from the fact that at the transition to an inverted hexagonal phase, the line tension of linear stalks is small. Thus as the architecture is varied such that the system approaches this transition, it must be inexpensive for the stalk to elongate and wander. That this is correct can be seen from the calculated line tension, λ_{ES}, of the elongated linear stalk shown in Fig. 16. It is essentially independent of tension, γ. We see that this line tension decreases with decreasing f as expected, which decreases the cost of elongating a stalk. The second condition is that the free energy of the hole which is created must not be too large. As noted earlier, the high cost of an isolated hole is due to the line tension of its periphery. If this is reduced by causing the hole to form next to the elongated stalk, as in Fig. 12 , the cost of the hole in the stalk-hole complex will also be reduced. To determine whether this is so, we have calculated the line tension of an isolated hole in a bilayer, λ_H, and also the line tension of a hole created next to an elongated stalk, λ_{SH}. These results, again essentially independent of the membrane tension, are shown in Fig. 16, as a function of architecture. It is seen that in the region of f in which successful fusion is possible, $0.29<f<0.37$, (see Fig. 14), the line tension of the hole is reduced by about a factor of two. Let us now show that even such a relatively small change can have a very large effect on the rate of fusion.

Consider the simple estimate of the free energy of a hole,

$$F_H = 2\pi\lambda_H R - \pi\gamma R^2. \tag{20}$$

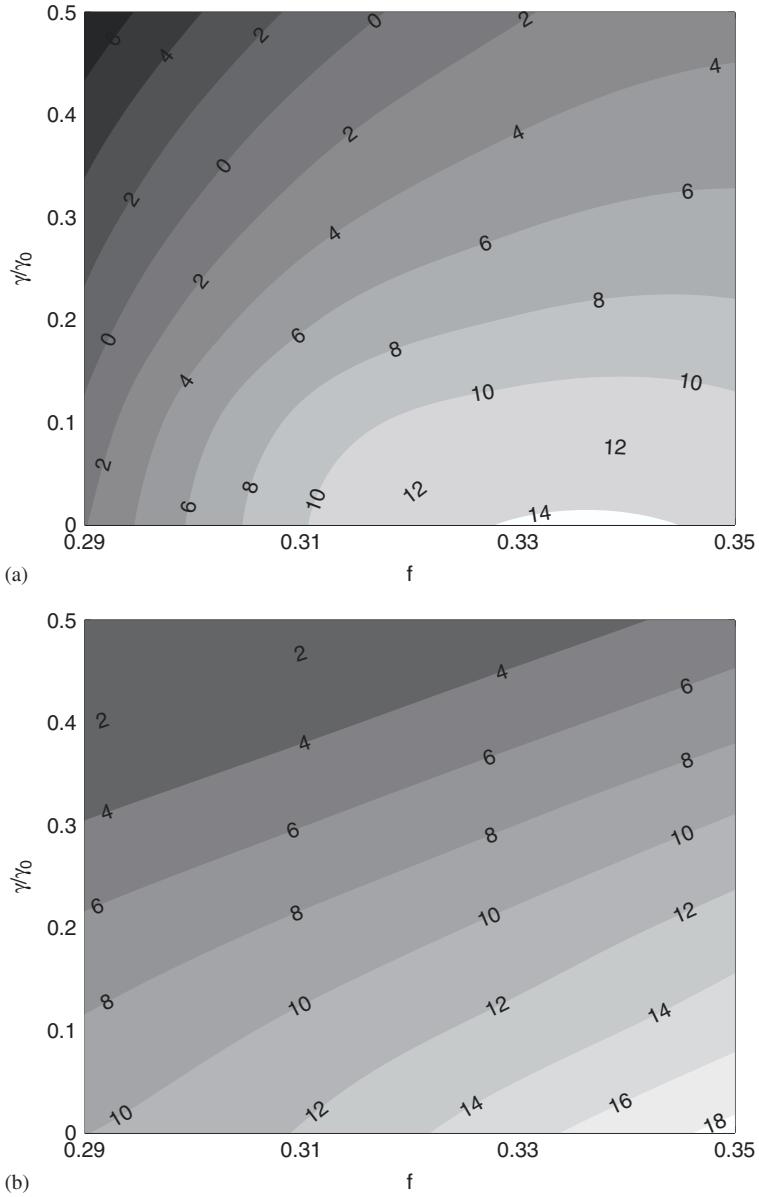

Fig. 15. Free energy barriers measured relative to the initial metastable stalk, in units of k_BT, in (a) the new stalk-hole complex mechanism, and (b) the standard hemifusion mechanism. Figure from Ref. [28].

The height of the barrier to stable hole formation corresponds to the maximum of this function. We ignore any R-dependence of λ_H and γ and immediately obtain the radius of the hole corresponding to the barrier to be $R^* = \lambda_H/\gamma$, and the height of the barrier to be $F^* = \pi\lambda_H^2/\gamma$. The rate of formation of an isolated hole in a bilayer is proportional to the Boltzmann factor

$$P_H = \exp\{-[F^* - k_BT\ln(A_H/\ell^2)]/k_BT\} \tag{21}$$

$$= \frac{A_H}{\ell^2}\exp(-\pi\lambda_H^2/\gamma k_BT), \tag{22}$$

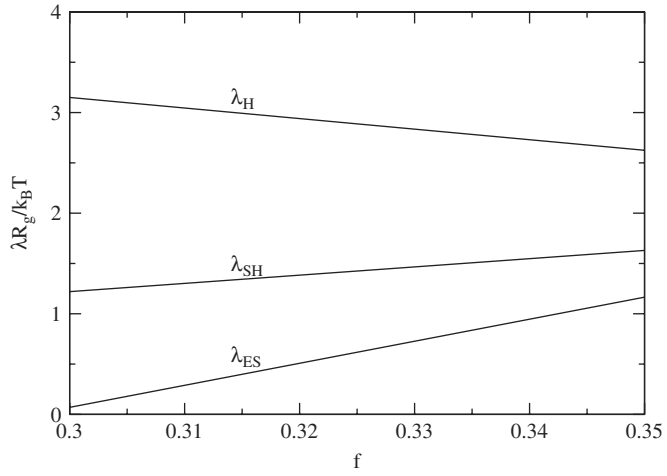

Fig. 16. Line tensions of a linear, extended, stalk, λ_{ES}, of a bare hole in a membrane, λ_H, and of a hole which forms next to a stalk, λ_{SH}. All line tensions are in units of k_BT/R_g. Figure from Ref. [28].

where the entropy associated with the formation of a hole in an available area A_H is $-k_B \ln(A_H/\ell^2)$ with ℓ a characteristic length on the order of the bilayer width. If $P_H \ll 1$, then the bilayer is stable to hole formation by thermal excitation.

The formation of the stalk-hole complex reduces the line tension of that part of the hole near the stalk from λ_H to λ_{SH}. This can be described by introducing the effective average line tension

$$\lambda_H \to \bar{\lambda}_\alpha \equiv \alpha\lambda_{SH} + (1-\alpha)\lambda_H. \tag{23}$$

Then the corresponding rate of stalk-hole complex formation becomes

$$P_{SH} = \frac{N_S a_S}{\ell^2} \exp(-\pi\bar{\lambda}_\alpha^2/\gamma k_B T), \tag{24}$$

where N_S is the number of stalks formed in the system and a_S is the area around each stalk in which hole nucleation can take place. For the small reduction $\lambda_{SH}/\lambda_H = \frac{1}{2}$, the above becomes

$$\frac{P_{SH}}{P_H} = \frac{N_S a_S}{A_H} \exp\left\{\frac{\pi\lambda_H^2}{\gamma k_B T}\left[\alpha\left(1-\frac{\alpha}{4}\right)\right]\right\} \tag{25}$$

$$= \frac{N_S a_S}{A_H}\left(\frac{A_H}{\ell^2 P_H}\right)^{\alpha(1-\alpha/4)}. \tag{26}$$

This shows explicitly that *if* the isolated membrane is stable to hole formation, (i.e., $P_H \ll 1$), *then* even a small reduction in the line tension ensures that formation of the stalk/hole complex causes the rate of hole formation in the apposed bilayers, and therefore fusion, to increase greatly.

We illustrate this with two examples. We first consider the copolymer membranes which we simulated previously [30,32]. In that case the exponent in the Boltzmann factor

$$-\frac{\pi\lambda_H^2}{\gamma k_B T} = -\pi\left(\frac{\lambda_H R_g}{k_B T}\right)^2\left(\frac{\gamma_0}{\gamma}\right)\left(\frac{k_B T}{\gamma_0 R_g^2}\right), \tag{27}$$

where γ_0 is the tension of an interface between bulk hydrophilic and hydrophobic homopolymer phases. The various factors in the simulated system are $\lambda_H R_g/k_B T = 2.6$ at $f = 0.35$, and $\gamma_0/\gamma = \frac{4}{3}$, $k_B T/\gamma_0 R_g^2 = 0.31$, $A_H/\ell^2 = 39$ [30,32]. Note that in the simulations multiple stalks have occasionally been observed. From this we obtain $P_H \approx 6 \times 10^{-3}$, so that isolated bilayers should have been stable to hole formation, as was indeed the case. However in the presence of a stalk, the Boltzmann factor will be increased according to Eq. (26). If we assume that the elongated stalk enclosed one half of the perimeter of the hole when it appeared, (i.e., $\alpha = \frac{1}{2}$), and that $N_S a_S/A_H \sim 0.3$ (consistent with the simultaneous observation of multiple stalks in a small simulation

cell [30]), we find that $P_{SH}/P_H \sim 14$ so that the rate of hole formation should have increased appreciably as observed in the simulations. This increase is expected to be more dramatic in biological membranes. In that case we estimate the exponent of the Boltzmann factor, $-\pi\lambda_H^2/\gamma k_B T$, as follows. We take the line tension to be that measured in a stearoyloleoylphosphatidylcholine and cholesterol bilayer, $\lambda_H \approx 2.6 \times 10^{-6}$ erg/cm [35,36]. For the surface tension, we take an estimate of the energy released by the conformational change of four of perhaps six hemagglutinin trimers arranged around an area of radius 4 nm, each trimer giving out about $60 k_B T$ [37]. This yields an energy per unit area $\gamma \approx 20\,\mathrm{erg/cm^2}$. Thus $P_H = 1.7 \times 10^{-11}(A_H/\ell^2)$, which indicates that even subject to this large, local, energy per unit area, the membrane is quite stable to hole formation for vesicles of any reasonable size. However if we assume again that the line tension of the hole is reduced by a factor of two by being nucleated next to the elongated stalk, that the stalk extends halfway around the circumference of the hole, and the density of stalks is such that $N_S a_S/A_H = 0.3$, then the rate of hole formation is increased by

$$\frac{P_{SH}}{P_H} = 0.3\left(\frac{1}{1.7 \times 10^{-11}}\right)^{7/16} \sim 1 \times 10^4, \tag{28}$$

i.e., an increase of more than four orders of magnitude.

One should note the implications of this simple argument. Because the probability to form a stable hole depends *exponentially* on the *square* of the line tension, an isolated bilayer is guaranteed to be stable against hole formation for normal line tensions. However, it is precisely this same dependence which also ensures that the bilayer will be destabilized by hole formation due to any mechanism which even modestly reduces that line tension. From here it is only a short step to successful fusion.

Acknowledgments

I have been fortunate to work with stimulating and engaging people on these projects, and I wish to thank them here: Richard Elliott, Kirill Katsov, Sarah Keller, Xiao-jun Li, Marcus Müller, Igal Szleifer, and Sarah Veatch. I thank Joseph Indekeu and his co-organizers for the invitation to present this work, and for their warm hospitality. Lastly I am grateful to the National Science Foundation for its continuing support. In particular this work was supported by grants DMR9531161, DMR9876864, DMR0140500, and DMR0503752.

References

[1] S.M. Gruner, Stability of lyotropic phases with curved interfaces, J. Phys. Chem. 93 (1989) 7562–7570.
[2] S.W. Chui, M.M. Clark, E. Jakobsson, S. Subramaniam, H.L. Scott, Application of combined Monte Carlo and molecular dynamics methods to simulation of dipalmitoylphosphatidylcholine lipid bilayer, J. Comput. Chem. 20 (1999) 1153–1164.
[3] I. Szleifer, A. Ben-Shaul, W.M. Gelbart, Chain statistics in micelles and bilayers: effects of surface roughness and internal energy, J. Chem. Phys. 85 (1986) 5345–5358.
[4] P.J. Flory, Statistical Mechanics of Chain Molecules, Wiley-Interscience, New York, 1969.
[5] S.L. Singer, G.L. Nicholson, The fluid mosaic model of the structure of cell membranes, Science 175 (1972) 720–731.
[6] M. Edidin, The state of lipid rafts: from model membranes to cells, Annu. Rev. Biophys. Biomol. Struct. 32 (2003) 257–283.
[7] T.P.W. McMullen, R.N.A.H. Lewis, R.N. McElhaney, Cholesterol-phospholipid interactions the liquid-ordered phase and lipid rafts in model and biological membranes, Curr. Op. Colloid Interface Sci. 8 (2004) 459–468.
[8] S. Munro, Lipid rafts: elusive of illusive?, Cell 115 (2003) 377–388.
[9] K. Simons, D. Toomre, Lipid rafts and signal transduction, Nature Rev. Mol. Cell Biol. 1 (2000) 31–41.
[10] K. Simons, W.L.C. Vaz, Model systems, lipid rafts, and cell membranes, Annu. Rev. Biophys. Biomol. Struct. 33 (2004) 269–295.
[11] R.F.M. de Almeida, A. Fedorov, M. Prieto, Sphingomyelin/phosphatidylcholine/cholesterol phase diagram: boundaries and composition of lipid rafts, Biophys. J. 85 (2003) 2406–2416.
[12] C. Dietrich, L. Bagatolli, Z.N. Volovyk, N. Thompson, K. Jacobson, E. Gratton, Lipid rafts reconstituted in model membranes, Biophys. J. 80 (2001) 1417–1428.
[13] S.L. Veatch, S.L. Keller, Organization in lipid membranes containing cholesterol, Phys. Rev. Lett. 89 (2002) 268101.
[14] S.L. Veatch, S.L. Keller, Separation of liquid phases in giant vesicles of ternary mixtures of phospholipids and cholesterol, Biophys. J. 85 (2003) 3074–3083.

[15] J.H. Ipsen, G. Karlström, O. Mouritsen, H. Wennerström, M. Zuckermann, Phase equilibria in the phosphatidylcholine-cholesterol system, Biochim. Biophys. Acta. 905 (1987) 162–172.
[16] R. Elliott, K. Katsov, M. Schick, I. Szleifer, Phase separation of saturated and mono-unsaturated lipids as determined from a microscopic model, J. Chem. Phys. 122 (2005) 0449041–04490411.
[17] R. Elliott, I. Szleifer, M. Schick, Phase diagram of a ternary mixture of cholesterol and saturated and unsaturated lipids calculated from a microscopic model, Phys. Rev. Lett. 96 (2006) 098101-1–098101-4.
[18] M.R. Vist, J.H. Davis, Phase equilibria of cholesterol/dipalmitoylphosphatidylcholine mixtures: nuclear magnetic resonance and differential scanning calorimetry, Biochemistry 29 (1990) 451–464.
[19] I.M. Hafez, S. Ansell, P.R. Cullis, Tunable pH sensitive liposomes composed of mixtures of cationic and anionic lipids, Biophys. J. 79 (2000) 1438–1446.
[20] X.-J. Li, M. Schick, Theory of lipid polymorphism: application to phosphatidyletanolamine and phosphatidylserine, Biophys. J. 78 (2000) 34–46.
[21] M.W. Matsen, Self-consistent field theory and its applications, in: G. Gompper, M. Schick (Eds.), Soft Matter, vol. 1, Wiley-VCH Verlag, Berlin, GmbH, 2006, pp. 87–179.
[22] F. Schmid, Self-consistent field theories for complex fluids, J. Phys. Condens. Matter 10 (1998) 8105–8238.
[23] K. Gawrisch, V.A. Parsegian, D.A. Hadjuk, M.W. Tate, S.M. Gruner, N.L. Fuller, R.P. Rand, Energetics of a hexagonal-lamellar-hexagonal phase transition sequence in dioleoylphosphatidylethanolamine membranes, Biochemistry 31 (1992) 2856–2864.
[24] M.M. Kozlov, S. Leiken, R.P. Rand, Bending, hydration, and interstitial energies quantitatively account for the hexagonal-lamellar-hexagonal re-entrant phase transition in dioleoylphosphatidylethanolamine, Biophys. J. 67 (1994) 1603–1611.
[25] X.-J. Li, M. Schick, Theory of tunable pH-sensitive vesicles of anionic and cationic lipids or anionic and neutral lipids, Biophys. J. 80 (2001) 1703–1711.
[26] L.V. Chernomordik, M.M. Kozlov, Protein-lipid interplay in fusion and fission of biological membranes, Annu. Rev. Biochem. 72 (2003) 175–207.
[27] K. Katsov, M. Müller, M. Schick, Field theoretic study of bilayer membrane fusion: I. Hemifusion mechanism, Biophys. J. 87 (2004) 3277–3290.
[28] K. Katsov, M. Müller, M. Schick, Field theoretic study of bilayer membrane fusion: II. Mechanism of a stalk-hole complex, Biophys. J. 90 (2006).
[29] M.M. Kozlov, V.S. Markin, Possible mechanism of membrane fusion, Biofizika 28 (1983) 255–261.
[30] M. Müller, K. Katsov, M. Schick, New mechanism of membrane fusion, J. Chem. Phys. 116 (2002) 2342–2345.
[31] B.D. Discher, Y.-Y. Won, D.S. Ege, J.C.-M. Lee, F.S. Bates, D.E. Discher, D.A. Hammer, Polymersomes: tough vesicles made from diblock copolymers, Science 284 (1999) 1143–1146.
[32] M. Müller, K. Katsov, M. Schick, A new mechanism of model membrane fusion determined from Monte Carlo simulation, Biophys. J. 85 (2003) 1611–1623.
[33] V.A. Frolov, A.Ya. Dunina-Barkovskaya, A.V. Samsonov, J. Zimmerberg, Membrane permeability changes at early stages of influenza hemagglutinin-mediated fusion, Biophys. J. 85 (2003) 1725–1733.
[34] H. Noguchi, M. Takasu, Fusion pathways of vesicles: a Brownian dynamics simulation, J. Chem. Phys. 115 (2001) 9547–9551.
[35] J.D. Moroz, P. Nelson, Dynamically-stabilized pores in bilayer membranes, Biophys. J. 72 (1997) 2211–2216.
[36] D.V. Zhelev, D. Needham, Tension-stabilized pores in giant vesicles-determination of pore-size and pore line tension, Biochim. Biophys. Acta 1147 (1993) 89–104.
[37] M.M. Kozlov, L.V. Chernomordik, A mechanism of protein-mediated fusion: coupling between refolding of the influenza hemagglutinin and lipid rearrangements, Biophys. J. 75 (1998) 1384–1396.